Improved seismic diffraction velocity estimation with fixed-depth semblance analysis

Anthony M. Hoch, Julian Ivanov, Shelby L. Peterie, and Richard D. Miller, Kansas Geological Survey*

Summary

Accurate seismic velocity estimation is a crucial component of geophysical interpretation. Semblance analysis is an efficient tool to estimate seismic velocity but is often limited by uncertainty in the source wavelet shape as well as added complexity introduced by changes in velocity along the travel path of the arriving energy. This investigation shows that fixed-depth semblance analysis can reduce the effect of unknown parameters resulting in a more accurate estimation of seismic velocity.

Introduction

The analysis of semblance spectra for the determination of normal moveout velocity (Taner, 1969) provides the seismic interpreter with a significant improvement in characterization of the velocity model for the subsurface. The conventional method for velocity analysis requires scanning through a set of common-velocity NMO-corrected shot gathers looking for an appropriate value to flatten the target arrivals (Yilmaz, 2000). Semblance analysis provides a means to more quickly and precisely calculate the seismic ray path velocity compared to earlier methods. A variety of semblance methods have ben presented (Neidell, 1971) in order to fine-tune the sensitivity of the analysis to noise and multi-path arrivals. After more than 30 years of research, we still find that velocity mode conversion and multiple arrivals (Verm, 2006) are still limitations to the accurate estimation of subsurface velocity.

This work will show that it is not always necessary to consider the presence of uncertainty and noise as a limitation to the semblance approach. Instead, by adjusting the geometric representation of the semblance information we can significantly reduce sensitivity to some parameters while at the same time using others to our benefit. Considering a fixed-depth value for the semblance plot we calculate the hyperbolic arrival of the seismic energy based on the velocity from the subsurface diffraction to the geophone locations within the receiver array. This method can determine, but does not require, specific detail relating to the velocity of the energy traveling to the diffraction point. Arrivals from multiple ray path geometries and velocity mode conversions aid in velocity estimation due to fitting the same hyperbolic shape as the primary arrival of that velocity. By emphasizing on the arrival velocity, the fixed-depth semblance model improves accuracy of the velocity estimation, while at the same time avoiding limitations present in standard semblance model analysis.

Synthetic Seismic Model

Synthetic seismic records were calculated using a finite-difference modeling utility developed at the Kansas Geological Survey (Zeng et al., 2011)). The model used for this analysis simulates a roll-along survey being collected over an air-filled tunnel at a depth of 10 meters below the surface (Table 1) and has been used to assess the feasibility of a wide variety of geophysical processing methods (Ivanov, 2017). A finite-difference grid is generated that is 450 meters wide and 45 meters deep. The air-filled void is centered 270.8 meters horizontally and 10.8 meters deep being 1.6 by 1.6 meters in size. The source wavelet used was the first derivate of the Gaussian with a peak frequency of 80 Hz.

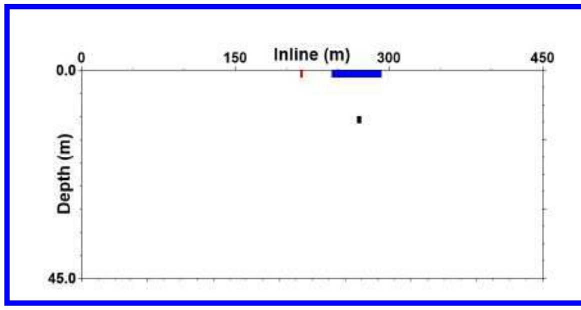

Figure 1. Schematic representation of the model geometry. The background is a single layer and the black rectangle is a diffraction point representing an air-filled cavity. The red and blue lines represent the locations of the source and receiver array for the record discussed in the text.

	Vs	*Vp*	*Density*
Background	500 m/s	1000 m/s	1.8 g/m^3
Void	0 m/s	343 m/s	0.001 g/m^3

Table 1. Model volume design properties.

Acquisition parameters for this model include 32 shot records consisting of 48 vertical receivers spaced at 1 meter intervals. The Source is located 30 meters from the first receiver and the array moves forward by two meters between each shot. For the sake of brevity, this analysis has been presented for a single record with the diffraction location near the center of the receiver spread (Figure 1). This record has the source location at station 5035 and the receiver locations between station 5065 and station 5112. The void location is centered nearest to station 5092.

10.1190/segam2018-2998596.1

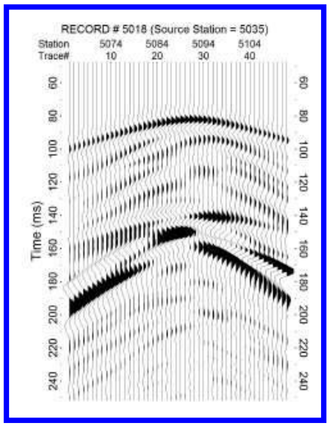

Figure 2. Time-Offset synthetic record showing various arrivals based on the model design.

Inspection of the time-offset record (Figure 2) shows that the energy diffracting from the void is the dominant energy in the record. Above 140 ms on the time axis shows multiple individual hyperbolic returns and below that region is a variety of overlapping returns.

Common-Velocity Analysis

Semblance analysis for diffraction is most often performed under the assumption that the velocity of the down-going energy is the same as the velocity of the up-going energy. If we overlay the expected hyperbolic arrivals for the two body wave velocities (Figure 3) we see that the record shows consistent hyperbolic returns for the PP and SS arrivals as well as a return that represents the mode converted PS wave. Since this converted mode arrival violates one of the assumptions of common-velocity semblance analysis we can expect that the energy will be misplaced and reduced in intensity on the semblance plot.

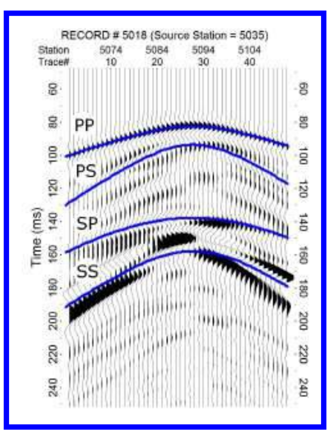

Figure 3. Time-Offset synthetic record showing hyperbolic projection of the four expected arrivals diffracting from the center location of the air-filled cavity.

Interpretation of the results on the semblance plot generated by processing this record (Figure 4) fits the expectations from the synthetic data time-offset record. The PP, SS, and PS arrivals are all present. The PS arrival is misplaced and diminished in magnitude compared to the other arrivals. The arrivals that are later in time show more spread in signal energy due to the variety of hyperbolic returns in that region of the record.

The portion of the analysis that is not immediately obvious on the semblance plot is that the calculated velocities are all misplaced. The synthetic seismic records were generated with a p-wave velocity of 1000 m/s and an s-wave velocity of 500 m/s but the location of the maximum values fall short of this by 6 to 12 percent (table 2). The cause for this drift in apparent velocity is that the peak energy is not located exactly at the beginning of the wavelet. Common-velocity semblance requires an adjustment for the difference in peak energy arrival to accurately predict body wave velocity, and this property is often not well estimated in during acquisition or understood during processing.

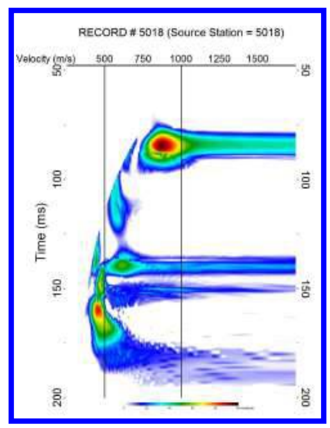

Figure 4. Semblance plot calculated using common-velocity assumptions. The vertical lines represent the seismic velocities used to generate the synthetic data. Both the PP and SS energy peaks are misplaced.

Mode	*Apparent*	*True*	*Error*
PP	876 m/s	1000 m/s	12.4 %
SS	470 m/s	500 m/s	6.0 %

Table 2. Calculated velocities based on the location of the maximum peak energy for the common-velocity semblance plot from Figure 4.

Fixed-Depth Analysis

Adjusting the semblance algorithm to use a fixed-depth of investigation, instead of a common-velocity, provides a way to estimate the velocity of the up-going energy independent of the peak energy time offset. This method also has the benefit of being independent of the velocity for the down-going energy. Energy traveling up from any diffraction point at the assumed diffraction location and depth will align with the same velocity along the horizontal axis. Adjusting the fixed-depth value shifts the peak locations from high to low as the depth used for the calculation is increased (Figure 5). At the correct depth all peaks will align vertically along the true body wave velocities. The center depth provided in our model is located at 10.8 meters, which correctly puts the true velocities slightly less that the values calculated for the depth of 10 meters (Table 3).

Fixed-depth semblance plots are less sensitive to uncertainty in the wavelet shape and can take advantage of this difference to more accurately estimate velocity. The peak energy time delay and the down-going velocity are included as part of the calculation to determine the time value on the vertical axis but the time of the energy peaks does not change significantly as the fixed-depth value is modified and is not considered a critical component to this method of investigation. The lack of sensitivity to the velocity of the down-going energy is an added benefit since the mode-converted arrivals appear on the semblance plot at a velocity based only on the up-going portion of their path.

Determination of diffraction depth and wave velocity based on the vertical alignment of multiple returns on a fixed-depth semblance plot provides the investigator with sufficient information to calculate the peak energy delay of the wavelet directly. At that point the common-velocity semblance algorithm can be adjusted to provide a common-velocity semblance plot that is more diagnostic of the subsurface environment (Figure 6) and velocity estimations that are more accurate (Table 4).

Mode	*0 m*	*5 m*	*10 m*	*15 m*	*20 m*
PP	1505m/s	1291m/s	105m/s	880m/s	728m/s
PS	1643m/s	1376m/s	1068m/s	822m/s	691m/s
SS	742m/s	680m/s	555m/s	480m/s	410m/s

Table 3. Calculated velocity for the peak maximum at three locations on the fixed-depth semblance plots.

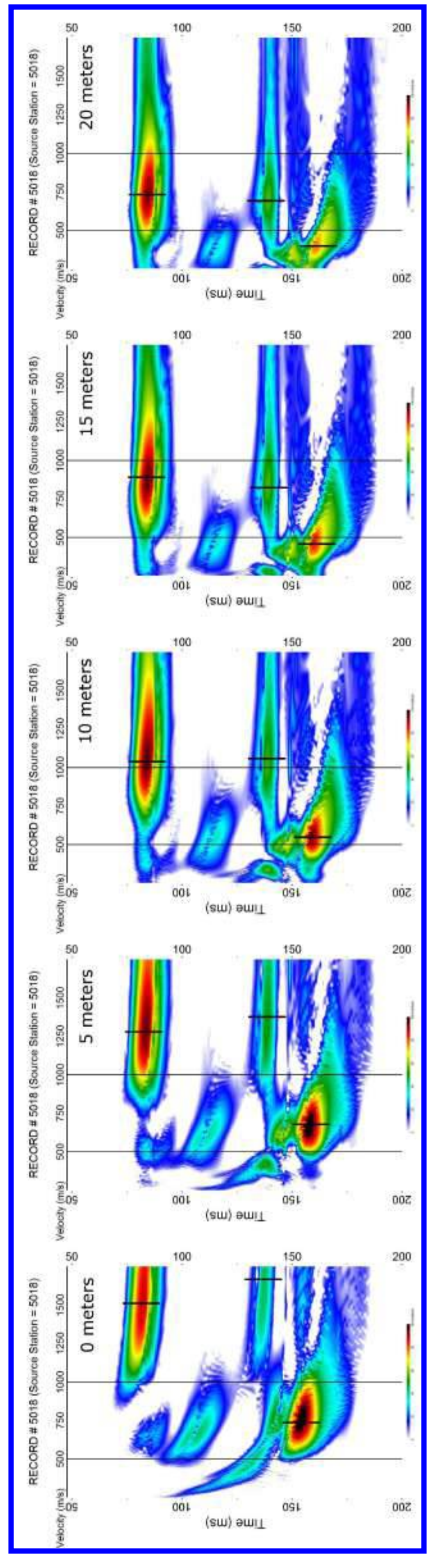

Figure 5. Five panel series of fixed-depth semblance plots. The lines at 500 m/s and 1000 m/s represent the true velocity of the model. The vertical black tick marks represent the location of the maximum for each of the three strongest peak energies.

10.1190/segam2018-2998596.1

Discussion

The projection of data displayed on a semblance plot relies extensively on the assumptions that have to be made. The common-velocity semblance method that is used for this project not only expects that the ray path follows diffraction geometry and that the down-going velocity is the same as the up-going velocity; but, each plot also assumes that the diffraction station is fixed and the wavelet peak delay time is known. In many cases this amount of a priori knowledge is beyond what is available at the time of interpretation. In order to provide more accurate velocity estimations we found that the effect of assumptions which are unknown at the time of acquisition are minimized by adjusting our algorithm to the geometry expected for the fixed-depth method.

The vertical axis for a fixed-depth semblance plot represents the time of arrival and is shifted based on the time of departure of the seismic energy from the point of the diffraction. Any change in the peak energy delay time of the down-going velocity results in a shift along this axis. Since the vertical axis is not used directly for determination of the up-going velocity we do not require accurate estimates of these parameters in order to calculate the velocity of the up-going energy that is represented along the horizontal axis.

Other methods of semblance can be used that consider a different set of assumptions in order to generate the final plot. One option would be to assign a constant value to the down-going velocity and only consider the up-going velocity as the variable constraining the horizontal axis. We have found that these methods provide a benefit in only specific cases and in general suffer from the same limitations as common-velocity semblance methods. The fixed-depth method provides the greatest improvement in accuracy for situations where the common-velocity approach is lacking.

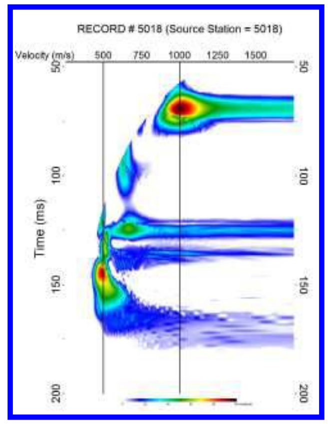

Figure 6. Common-velocity semblance plot after adjustment for wavelet peak energy delay. The maximum representing the PP and SS arrival fit the expected model values. The PS arrival is still misplaced on this plot due to violating the common-velocity assumption.

Mode	*Apparent*	*True*	*Error*
PP	1003 m/s	1000 m/s	0.3 %
SS	494 m/s	500 m/s	1.2 %

Table 4. Calculated velocity for peak maximums from the common-velocity semblance plot after adjustment.

Conclusions

Attaining accurate seismic body wave velocities is one of the most common reasons for considering semblance analysis as part of a processing routine. Uncertainty in wavelet shape and interference from mode-converted arrivals make common-velocity semblance more difficult to perform and reduce the resulting accuracy of velocity estimations. Using the fixed-depth semblance analysis method provides a more direct means of estimating body wave velocity that is not adversely affected by wavelet shape or velocity mode conversion.

10.1190/segam2018-2998596.1

REFERENCES

Ivanov, J., R. D. Miller, D. Z. Feigenbaum, and S. L. Peterie, 2017, Detecting subsurface objects and identifying voids possibilities using the back-scatter analysis of surface wave (BASW) method: International Conference on Engineering Geophysics, 116–119.

Neidell, N. S., and M. T. Taner, 1971, Semblance and other coherency measures for multichannel data: Geophysics, **36**, 482–497, https://doi.org/10.1190/1.1440186.

Taner, M. T., and F. Koehler, 1969, Velocity spectra - Digital computer derivation and applications of velocity functions: Geophysics, **34**, 859–881, https://doi.org/10.1190/1.1440058.

Verm, R. W., and W. W. Symes, 2006, Practice and pitfalls in NMO based differential semblance velocity analysis: 76th Annual International Meeting, SEG, Expanded Abstracts, 2112–2116, https://doi.org/10.1190/1.2369954.

Yilmaz, O., 2000, Seismic data analysis: SEG.

Zeng, C., J. H. Xia, R. D. Miller, and G. P. Tsoflias, 2011, Application of the multiaxial perfectly matched layer (M- PML) to near-surface seismic modeling with Rayleigh waves: Geophysics, **76**, no. 3, T43–T52, https://doi.org/10.1190/1.3560019.

10.1190/segam2018-2998596.1